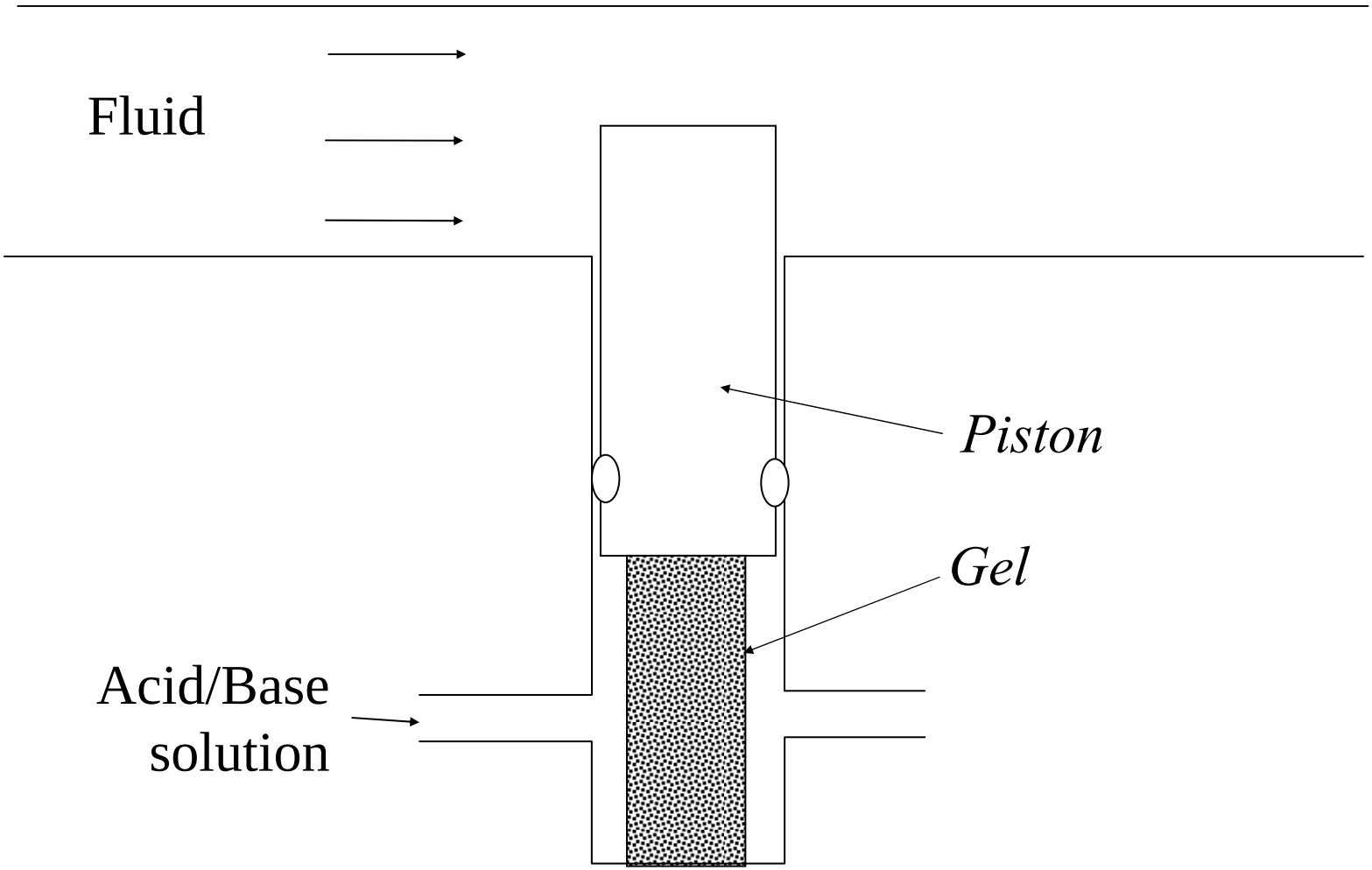

Figure 24.1 Similarities in function of actuators with conventional pistons.

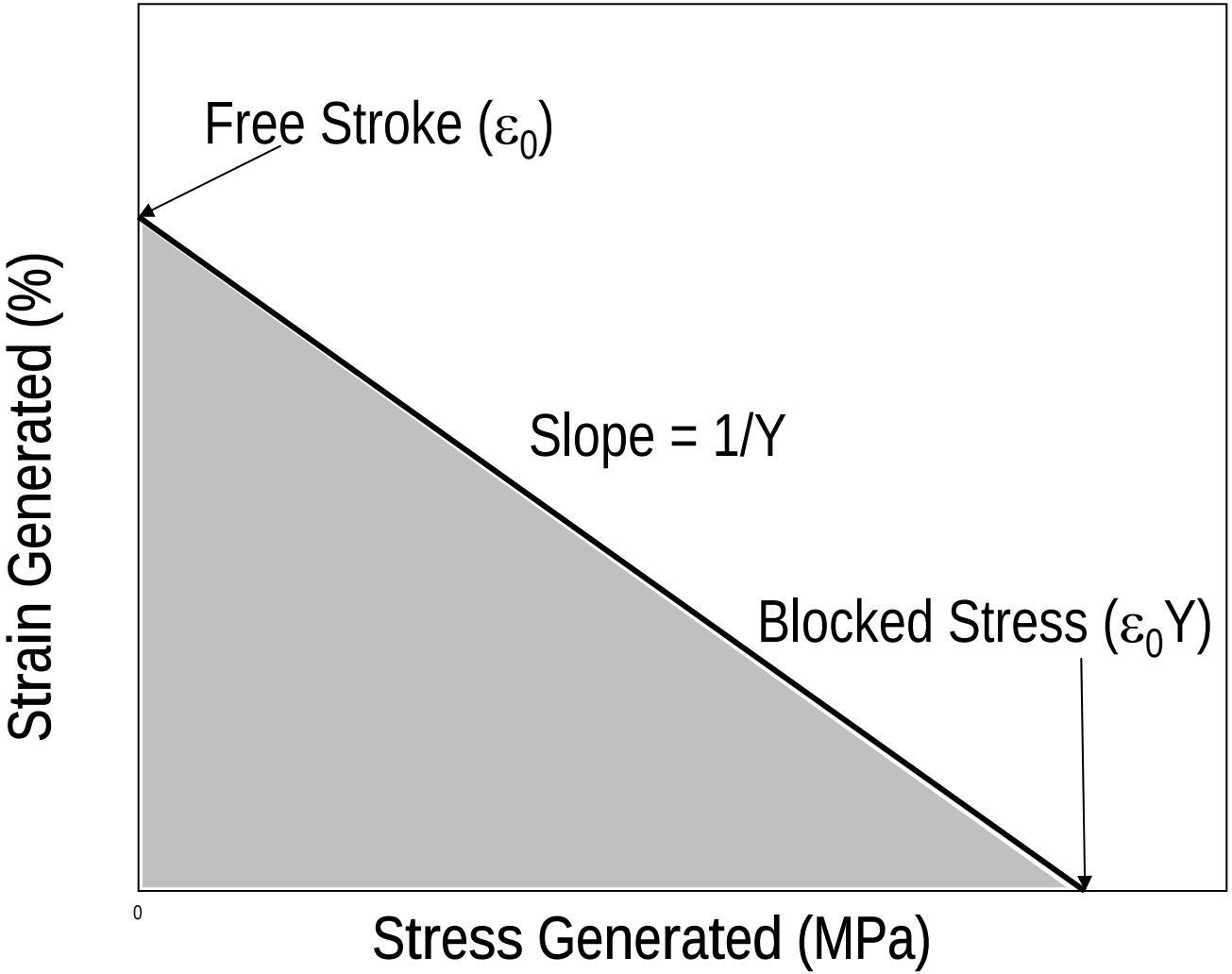

Figure 24.2 Schematic illustration showing how the stress and strain generated vary between the extremes of maximum strain (free stroke) at zero stress and maximum stress (blocked stress) at zero strain. Y is the Young's modulus of elasticity. The shaded area is the region in which the actuator can operate.

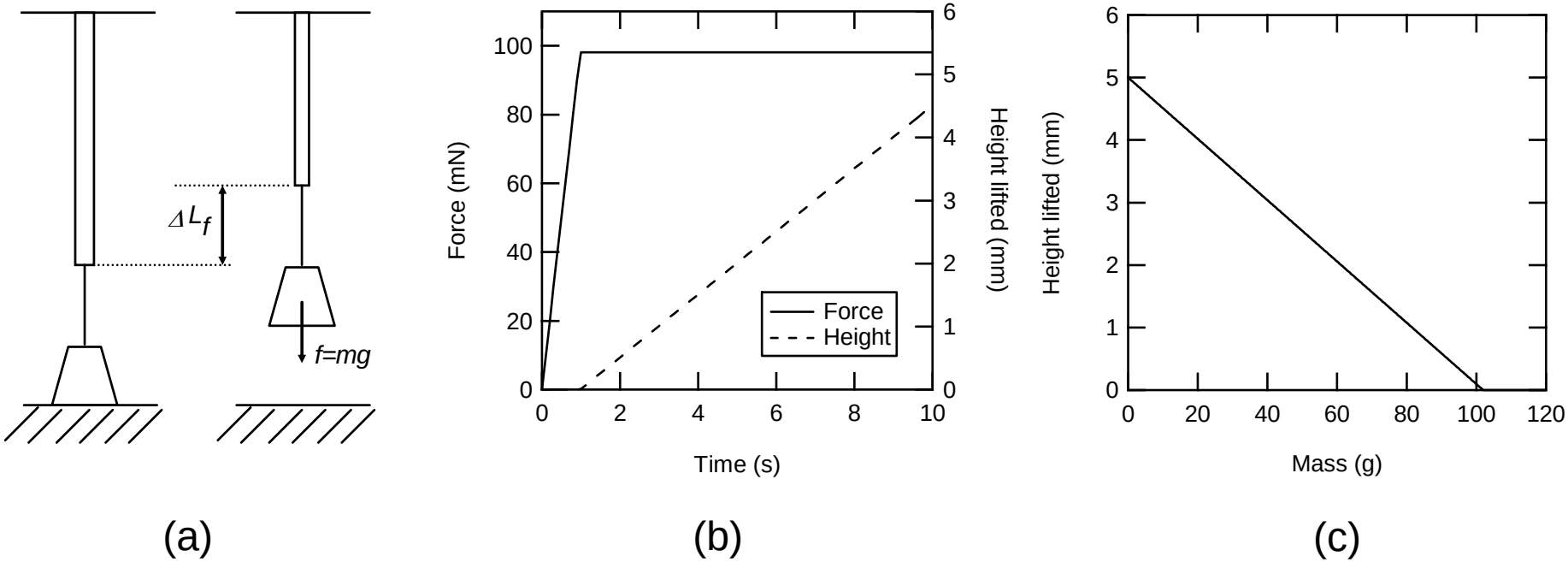

Figure 24.3 (a) Schematic diagram of a hypothetical actuator that generates a contractile free stroke (at zero load) of 10% attached to a weight of mass m. (b) Height that a mass of 10 g is lifted and force generated in the contractile actuator during the 10 s contraction of a 50 mm long actuator and 10 mm^2 cross-sectional area. (c) Final height (after full 10 s contraction) that the mass is lifted for different sized weights.

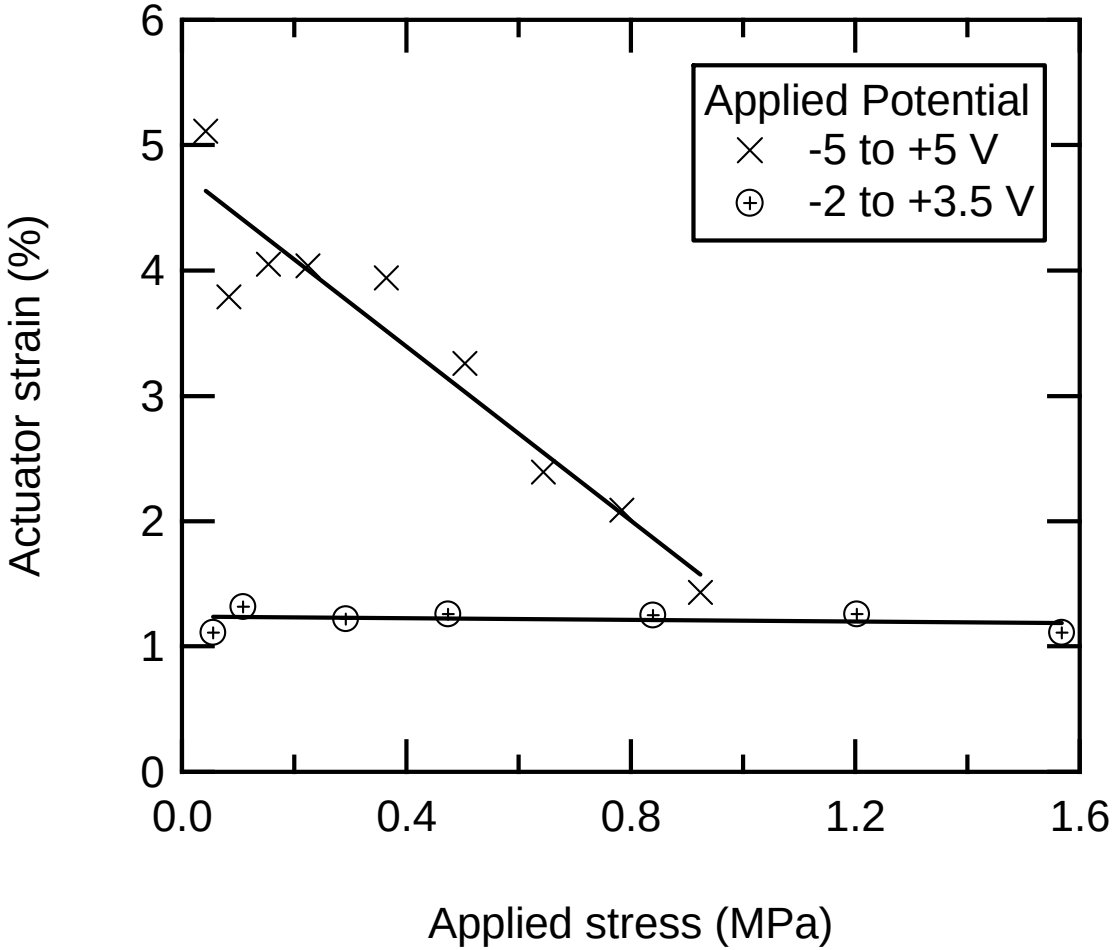

Figure 24.4 Measured isotonic strains for polypyrrole (PPy) actuators operated at different applied stresses (initial stretching caused by the application of the stress has been ignored[7]). (From Spinks, G.M., Liu, L., Wallace, G.G., and Zhou, D., Adv. Funct. Mater., 12, 437, 2002. With permission)

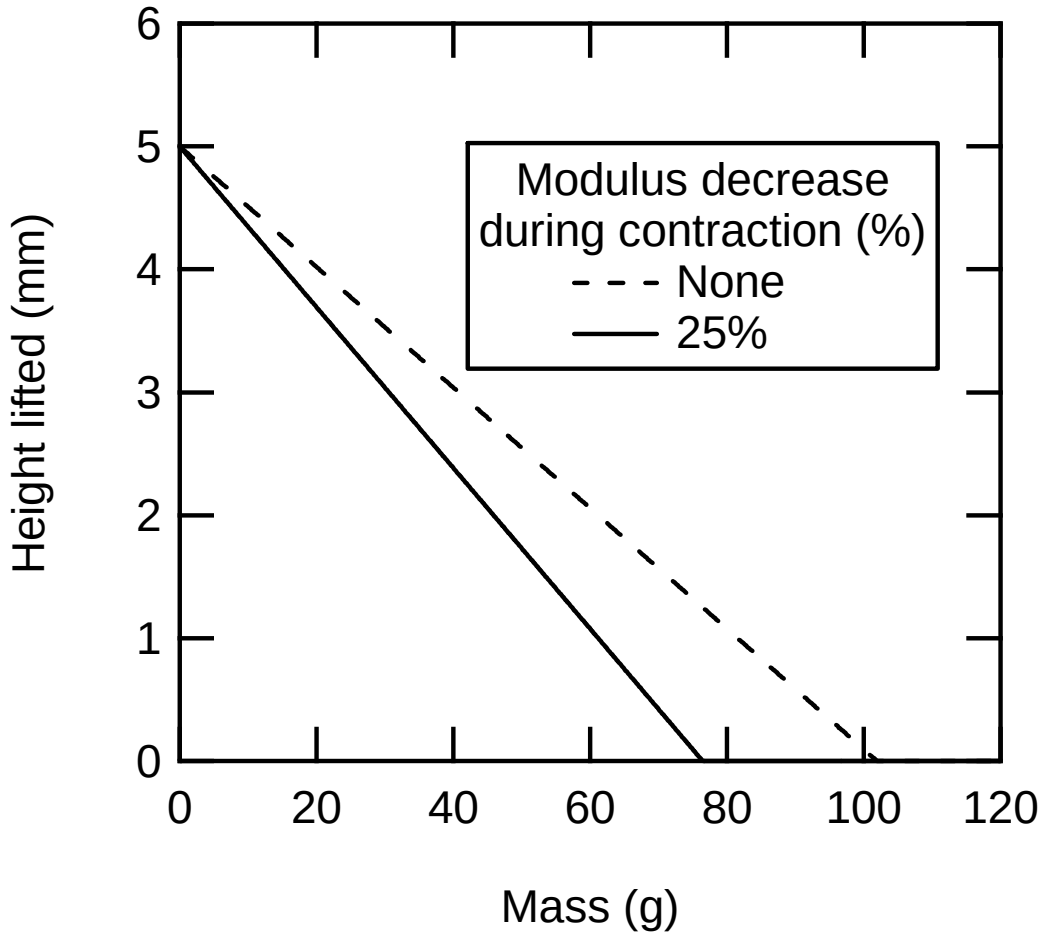

Figure 24.5 Height lifted by a contractile actuator (as in Figure 3) considering a 25% decrease in modulus during contraction – the dashed line shows the height lifted when there is no change in modulus.

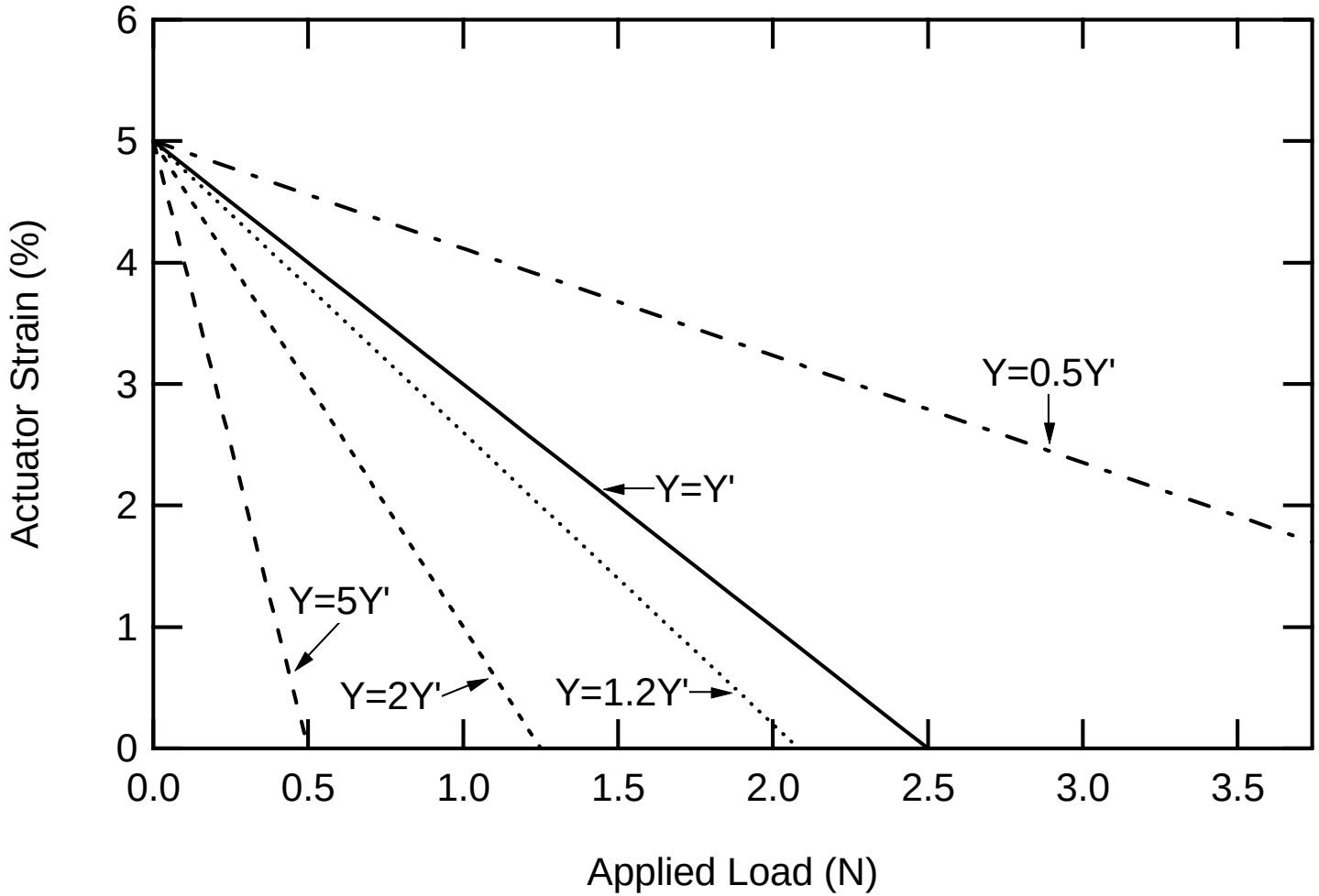

Figure 24.6 Calculated actuator strains at different applied loads for different ratios of expanded:contracted state moduli. Here the initial deformation caused by the application of load contributes to the net actuator strain.

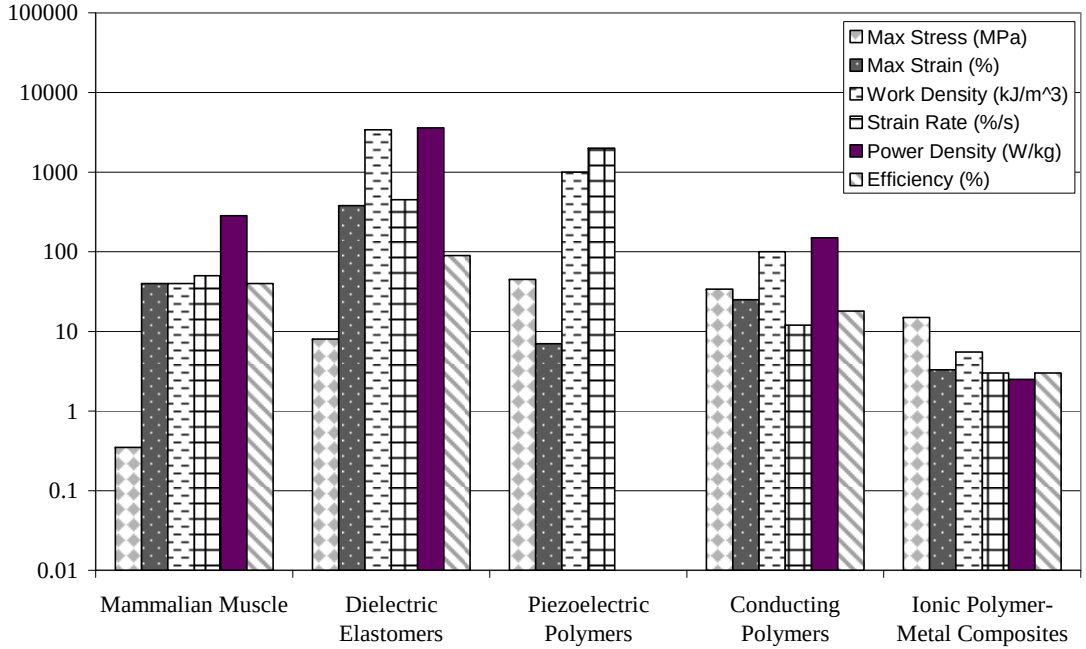

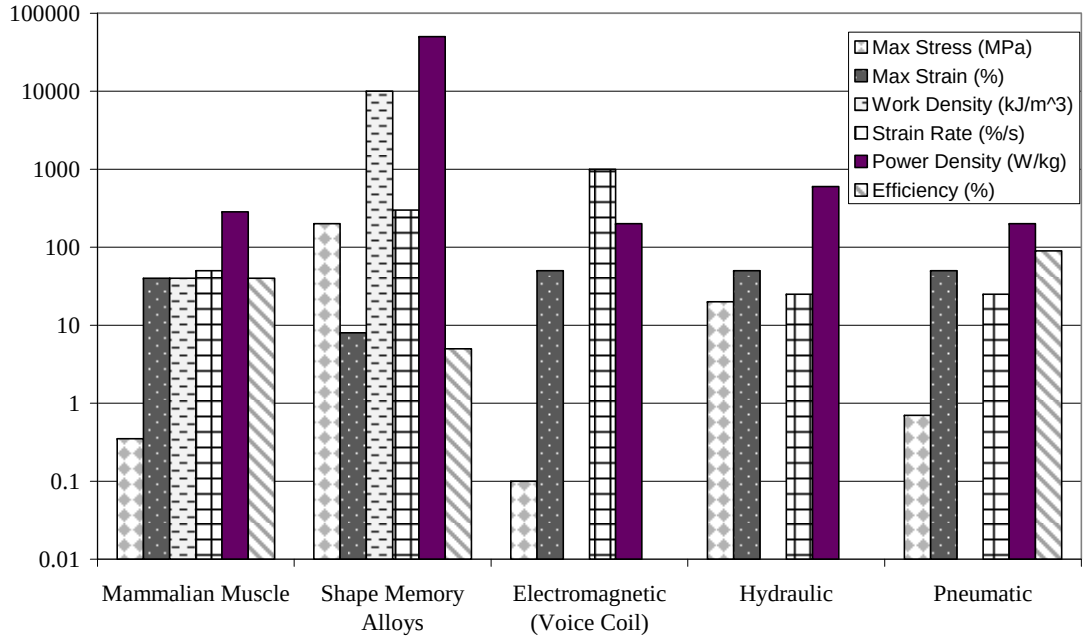

Figure 24.7 Comparative performance (current) of various actuators and mechanical drive systems.

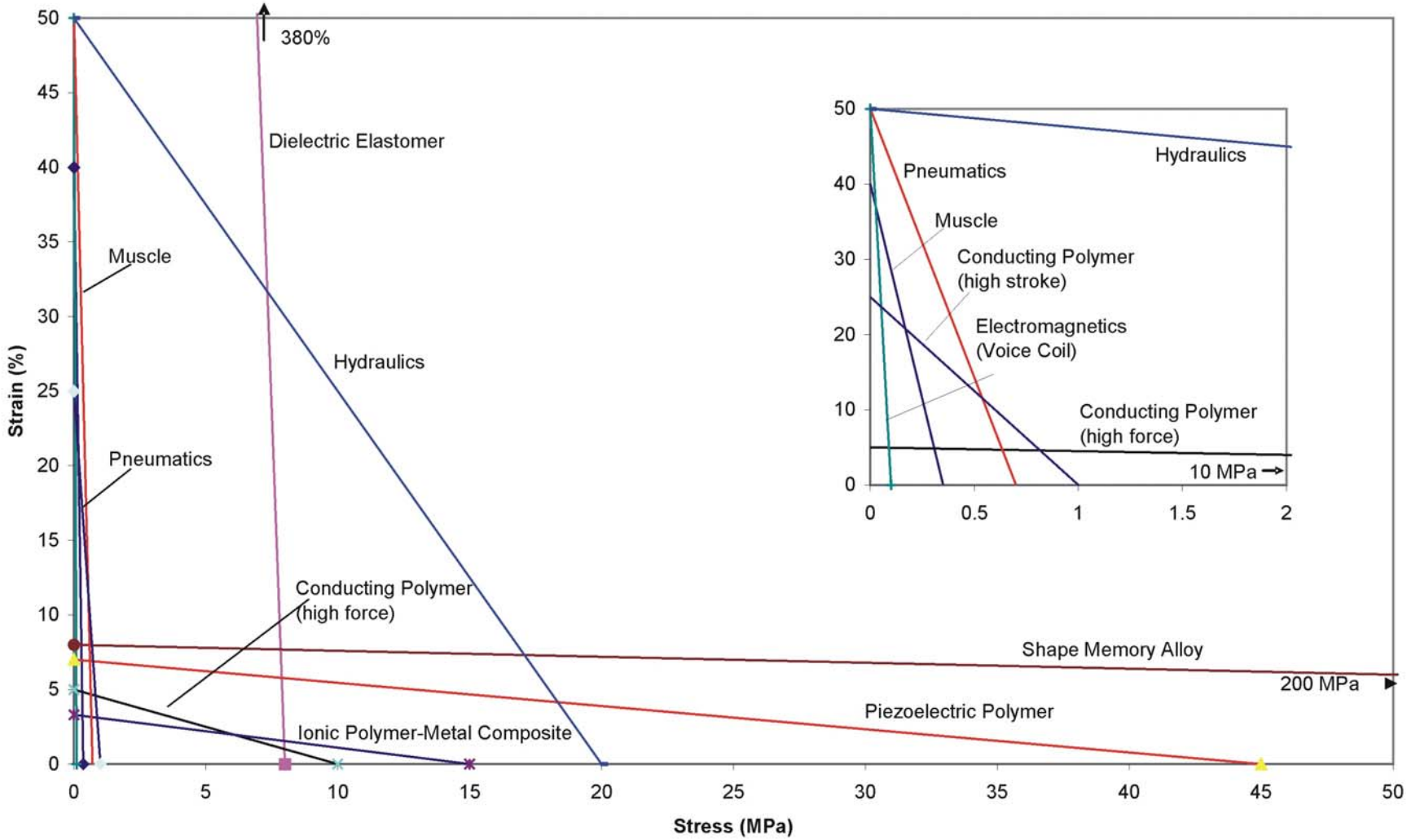

Figure 24.8 Strains at different applied stresses for various actuator materials and mechanical drive systems. The strain intercept is the free stroke and the stress intercept is the blocked stress. As described in Figure 24.2, the region below each line represents the region in which the actuator can operate.

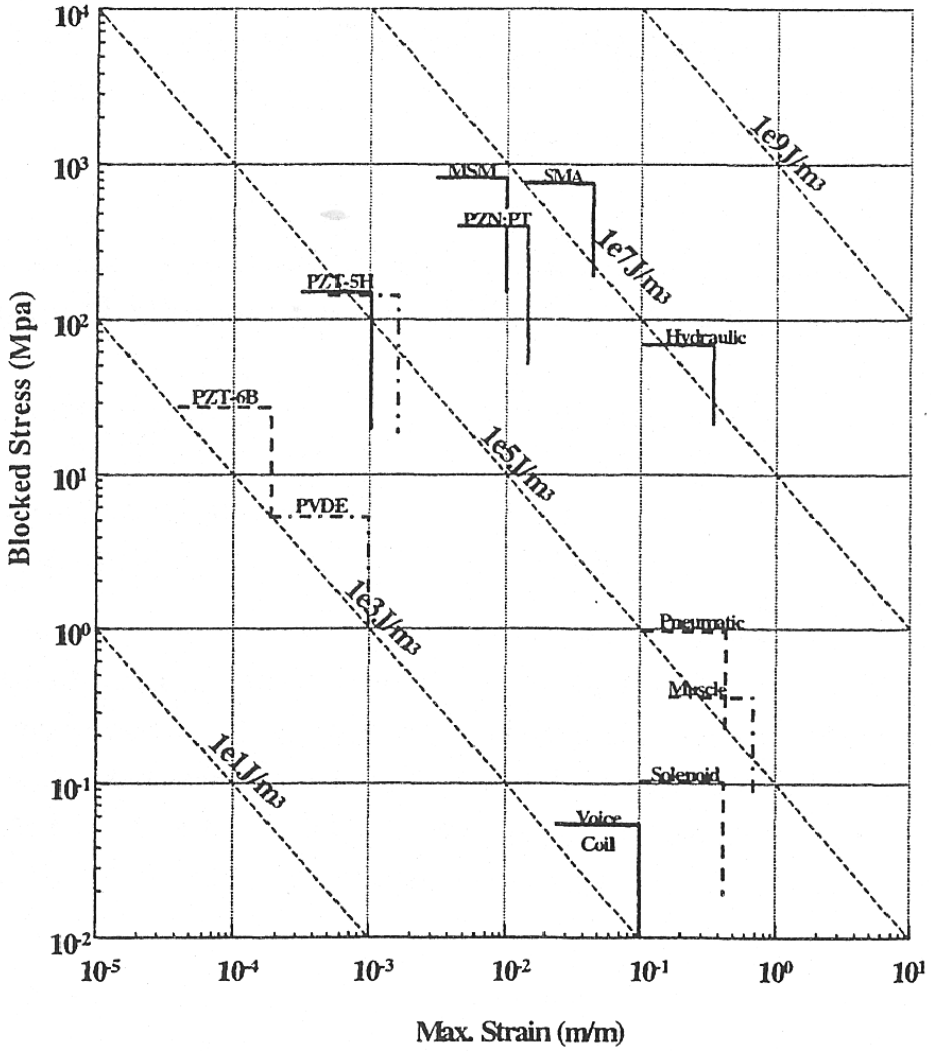

Figure 24.9 Comparison of stress and strains generated by various linear actuators. (From Wax, S. G. and Sands, R.R., Proc. SPIE-Int. Soc. Opt. Eng., 3669, 2, 1999. With Permission.) The maximum strain and blocking stress are defined in Figure 24.2.

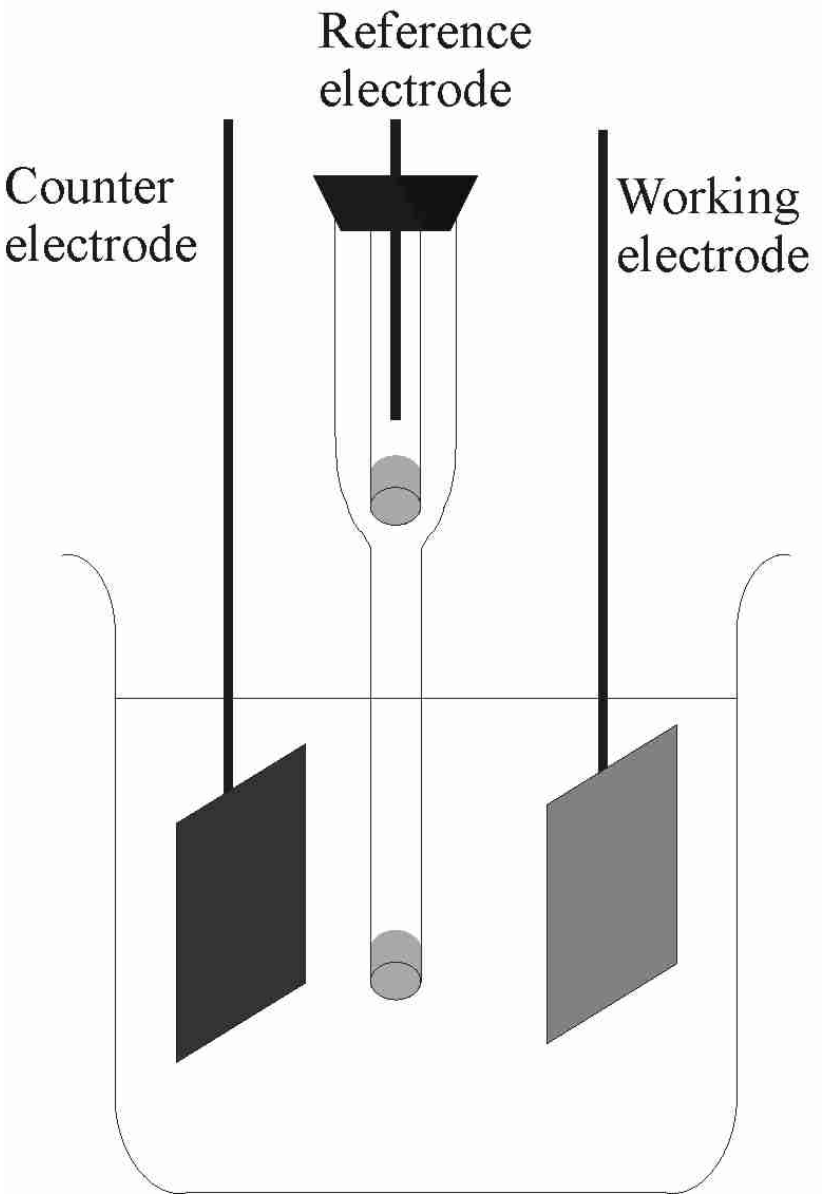

Figure 24.10 Electrochemical cell arrangement used for conducting polymer actuators. In some configurations the counter electrode is also the reference electrode [7]. (From Spinks, G.M., Liu, L., Wallace, G.G., and Zhou, D., Adv. Funct. Mater., 12, 437, 2002. With permission)

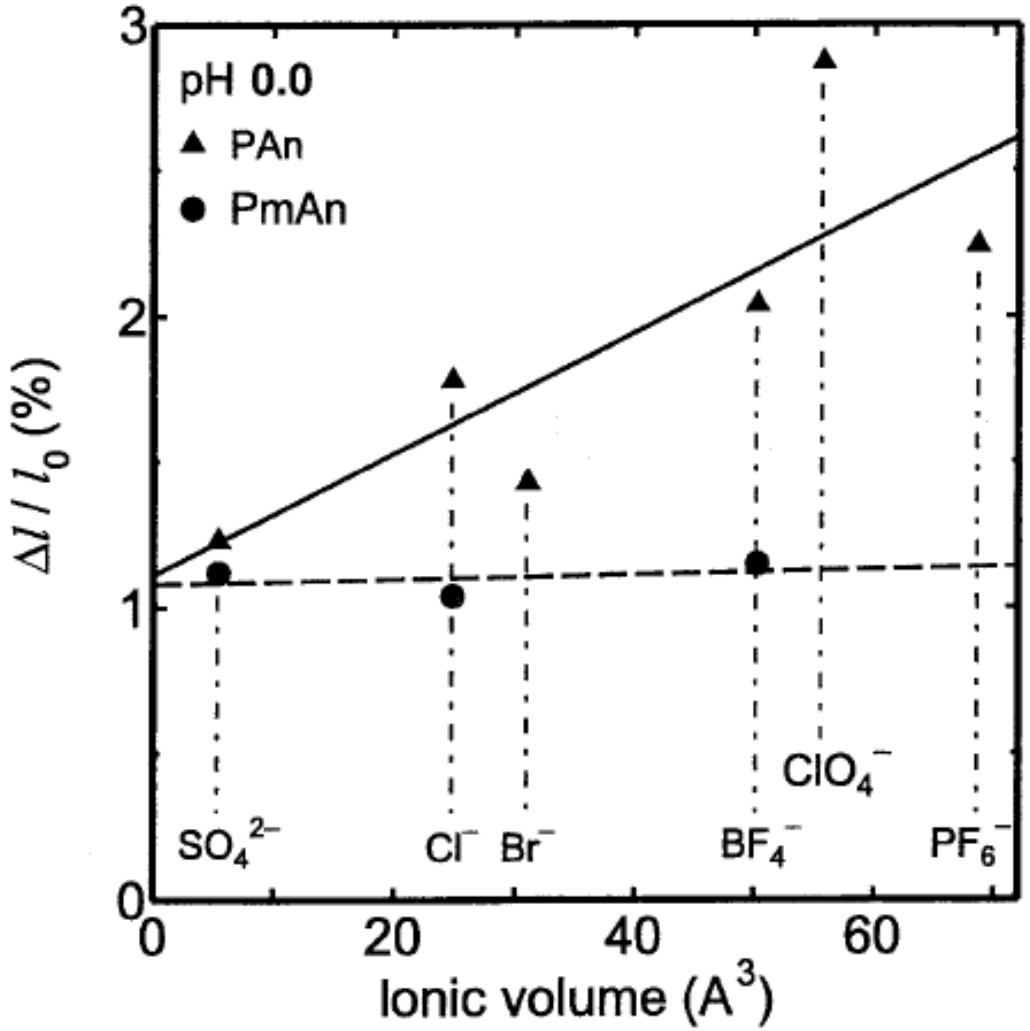

Figure 24.11 Actuator strain versus anion size for PANi. (Taken from Keneto, K. and Kaneko, M., Appl. Biochem. Biotechnol., 96, 13, 2001. With permission.)

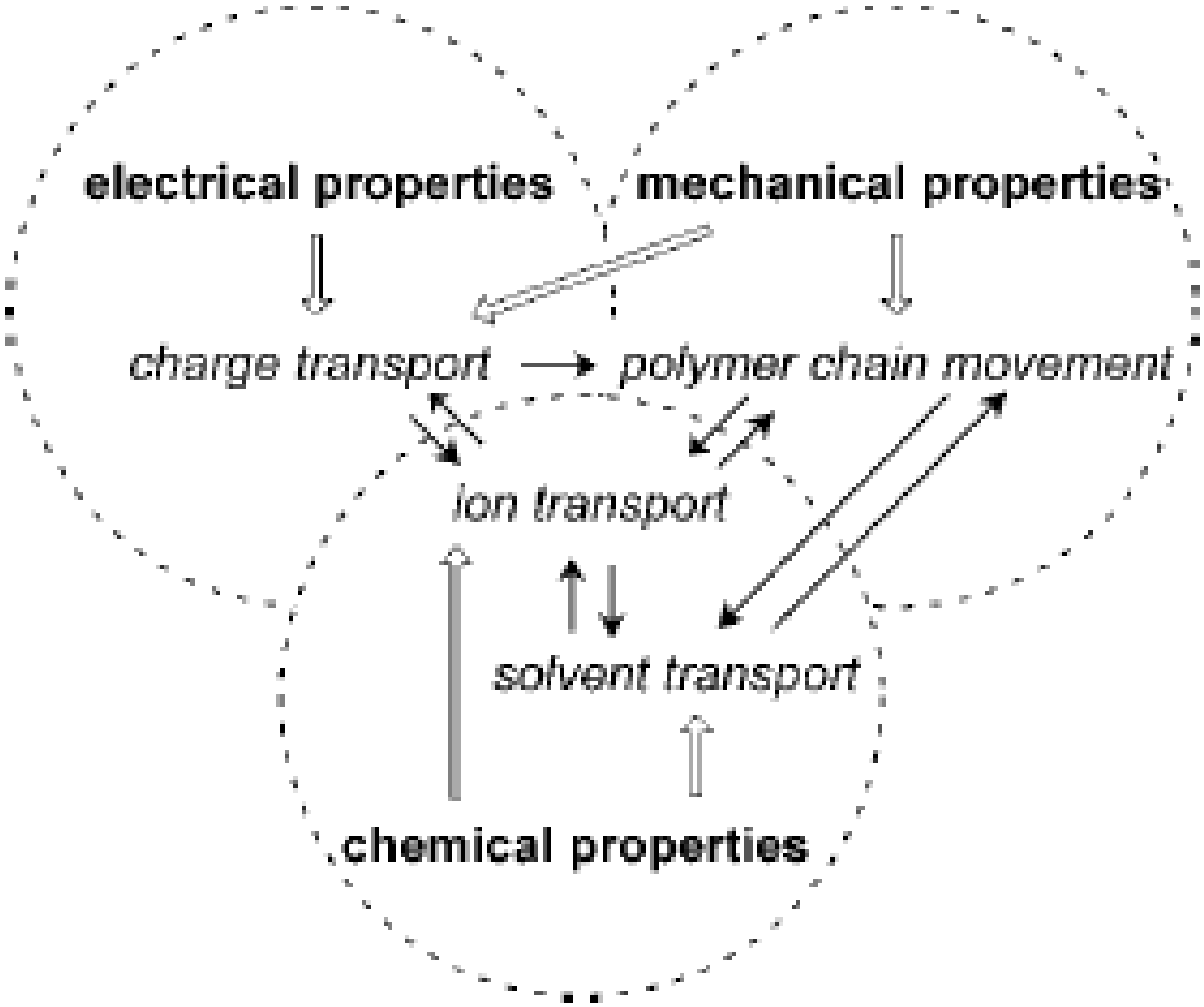

Figure 24.12 The inter-relationship of electrical, mechanical and chemical properties of conducting polymers [5]. (From Smela, E., Adv. Mater. (Weinheim, Germany), 15, 481, 2003. With permission.)

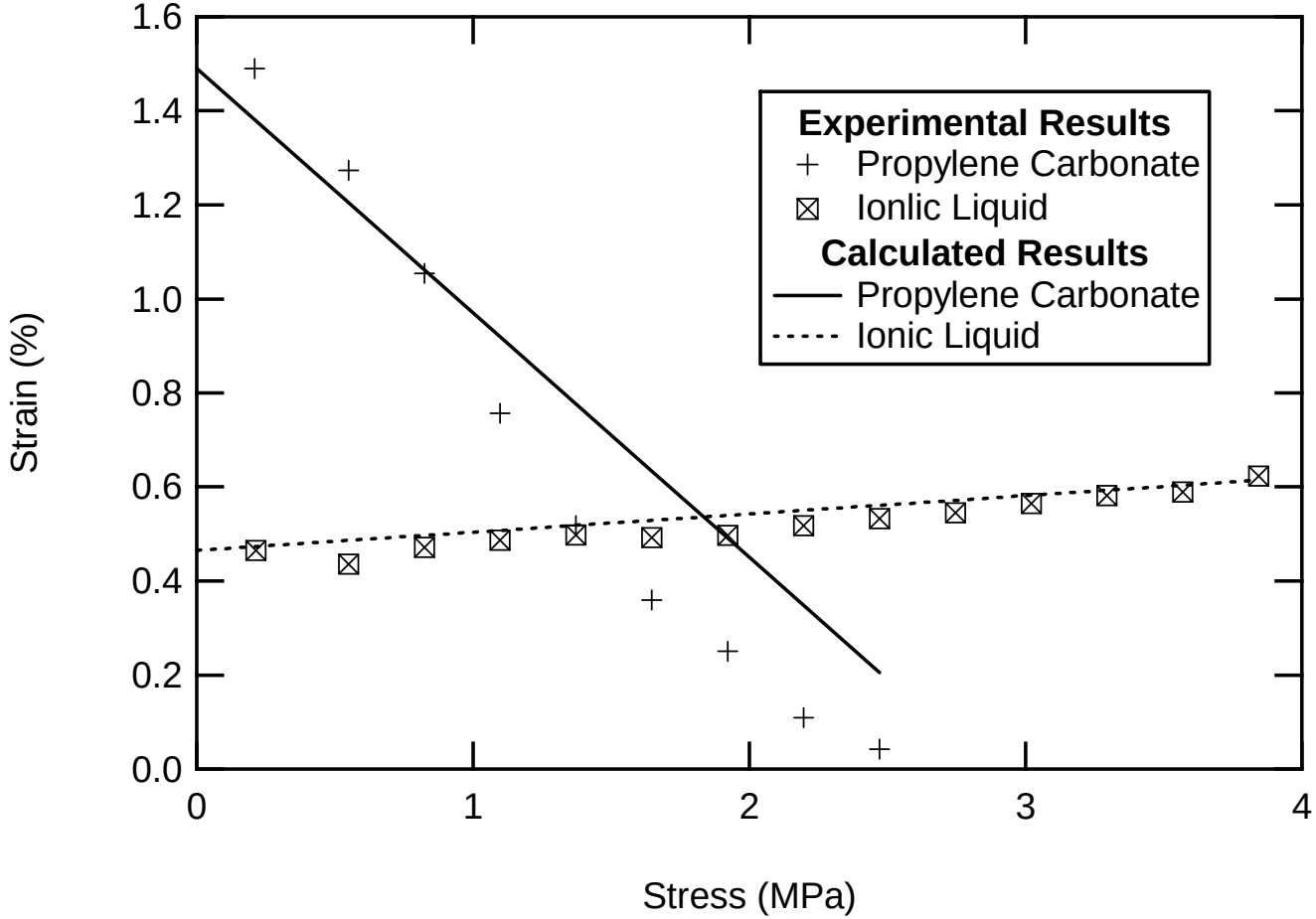

Figure 24.13 Actuation strain of a poly(3-methylthiophene) actuator doped with PF_6^- tested under isotonic conditions at different stress levels in both PC and ionic liquid electrolytes. Potential scanned between -1.0 to 1.5 V (vs Ag/Ag^+). The calculated strains obtained from Young's modulus modeling (Equation 24.3) are shown as dashed lines. (From Xi, B., Truong, V.-T., Whitten, P.G., Ding, J., Spinks, G.M., and Wallace, G.G., Polymer, 47, 7720, 2006. With permission.)

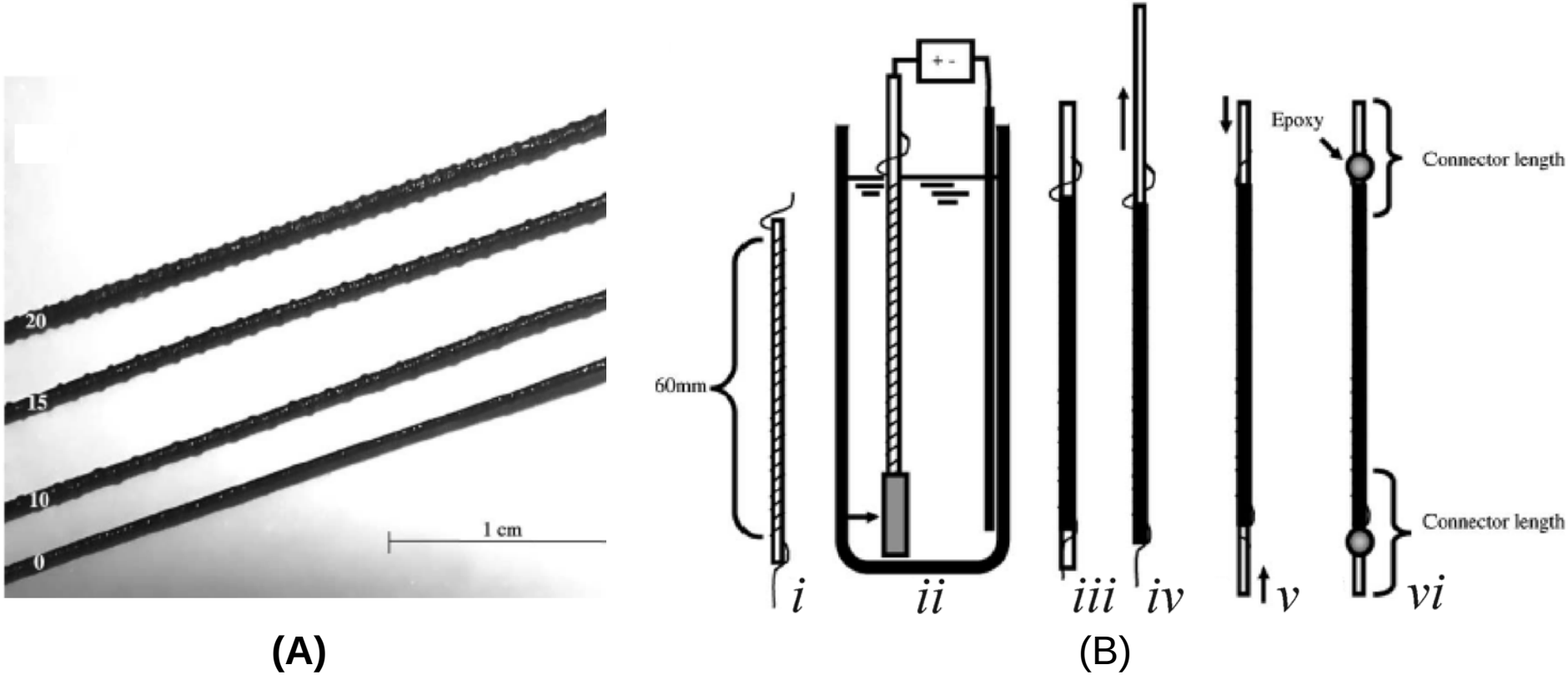

Figure 24.14 A helical wound platinum wire is used to minimize resistive losses. Photographs (A) of hollow polymer tubes with helical interconnect used for actuation testing. The pitch of the helix can be altered with examples shown of 20, 15 and 10 turns cm^{-1}. A hollow tube with no helix (0 turns cm^{-1}) is also shown. Schematic diagram (B) showing method of construction for these actuators; (i) 25 of platinum wire is wrapped around the 125 µm wire as a spiral; (ii) polymer synthesis—the assembly is placed in polymer electrolyte solution (0.5 M PPy, 0.25 M TBA PF_6 in PC) and electroplated for 24 hours at -28°C ; (iii) polymer coating forms around wire and spiral; (iv) 125 µm centre wire is withdrawn from the polymer tube/helix; (v) 2 short connectors of 125 µm wire are inserted into each end; (vi) 25 µm wire is pulled tight around these ends for a good electrical connection and epoxy glued to hold in place. (Taken from Ding, J., Liu, L., Spinks, G. M., Zhou, D., Wallace, G.G., and Gillespie, J., Synth. Met., 138, 391, 2003. With permission).

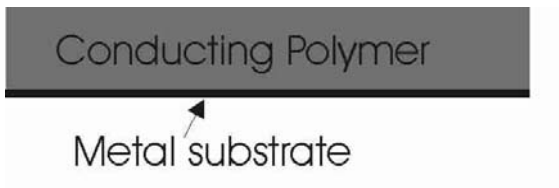

(A) A conducting polymer on top of a metal substrate.

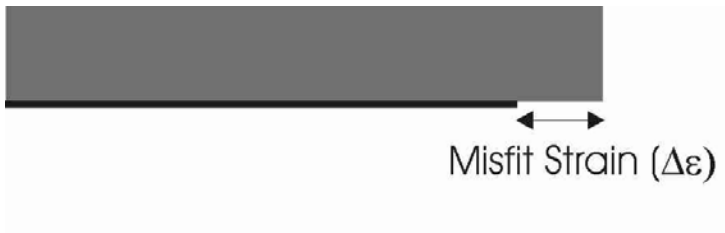

(B) The conductive polymer in A has expanded, but is not bonded to the substrate.

(C) The conductive polymer in A has expanded, and bends as a result due to being bound to the substrate.

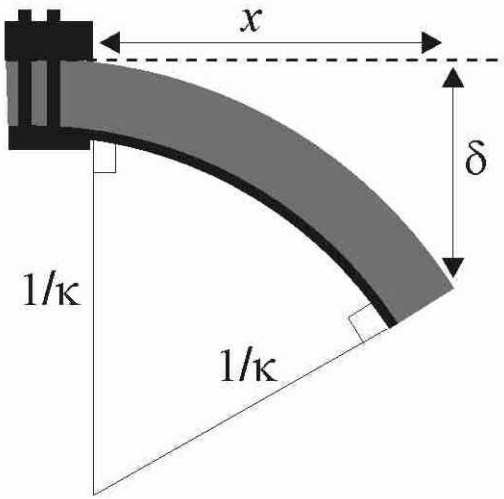

(D) Calculation of the bending curvature.

Figure 24.15 Volume change actuators can be used to make a bender by bonding onto a thin substrate of higher modulus. The misfit strain shown in (C) is equivalent to the free stroke produced by the actuator.

Figure 24.16 A "gripper" device constructed from multiple trilayer PPy benders.

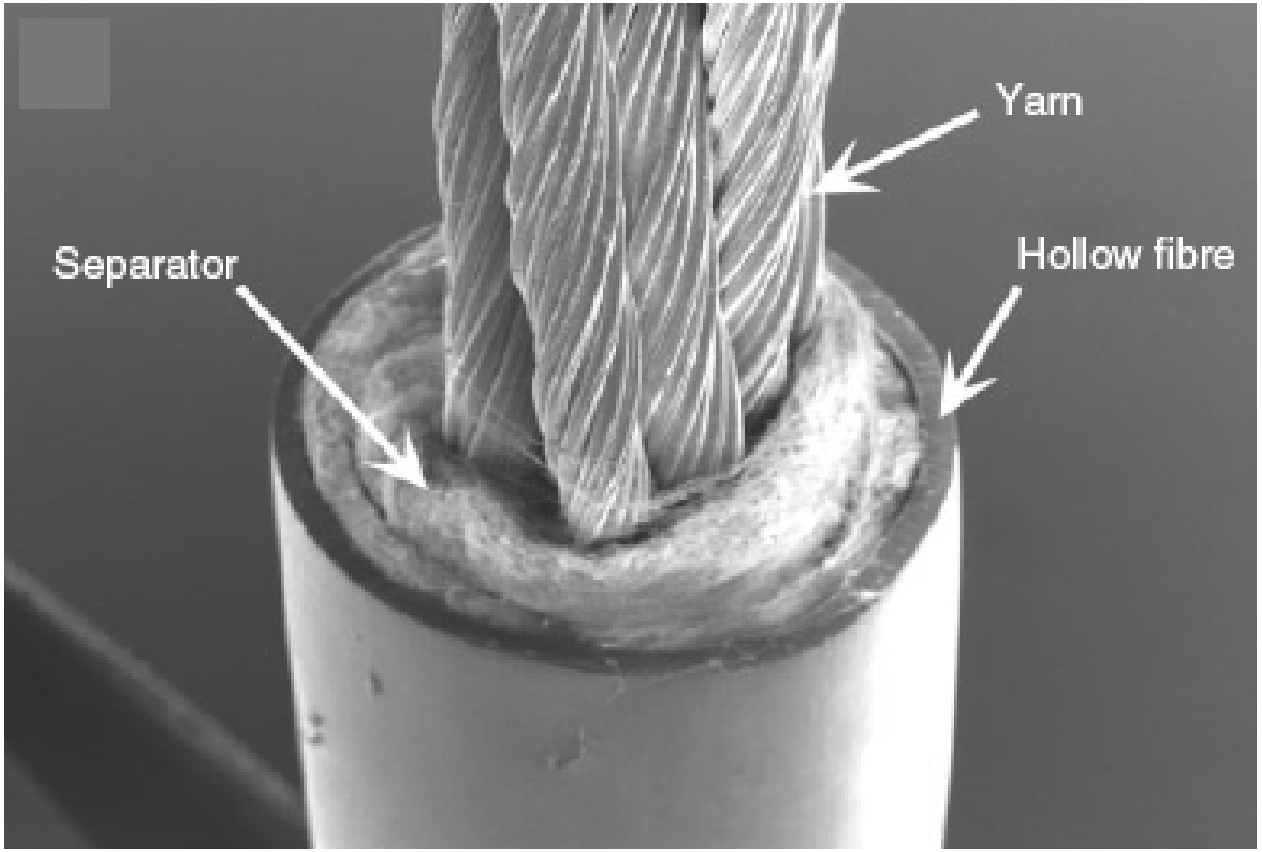

Figure 24.17 PANi fibres for high speed actuators, produced by Santa Fe Science and Technology [51], and presented in [50]. The diameter of the hollow fiber is 1.5 mm. (From Lu, W., Norris, I.D., and Mattes, B.R., Aust. J. Chem., 58, 263, 2005. With permission)

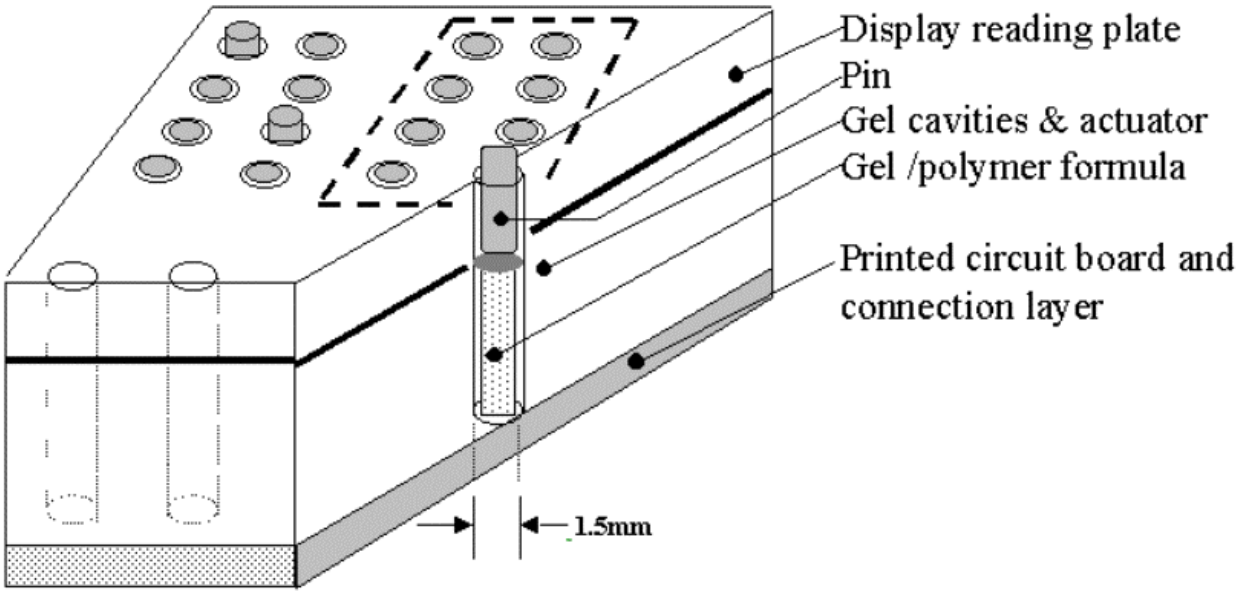

Each pin is

- individually addressed moves ~0.5mm in 0.2 s
- (1% strain and 5%/s strain rate)
- sits on a spring to provide tactile resistance
- (10 g_f depresses pin <0.1 mm, requiring a spring constant of 1000 N/m and a max. actuation force of > 0.5 N or >10 MPa stress for an actuator diameter of 0.05mm^2)
- lasts > 10^6 cycles

Figure 24.18 Design and specifications for an electronic Braille screen that is being developed by Quantum Technology Pty. Ltd. (From Quantum Technology Pty Ltd., 5 South Street (PO Box 390), Rydalmere, NSW 2116, Australia)

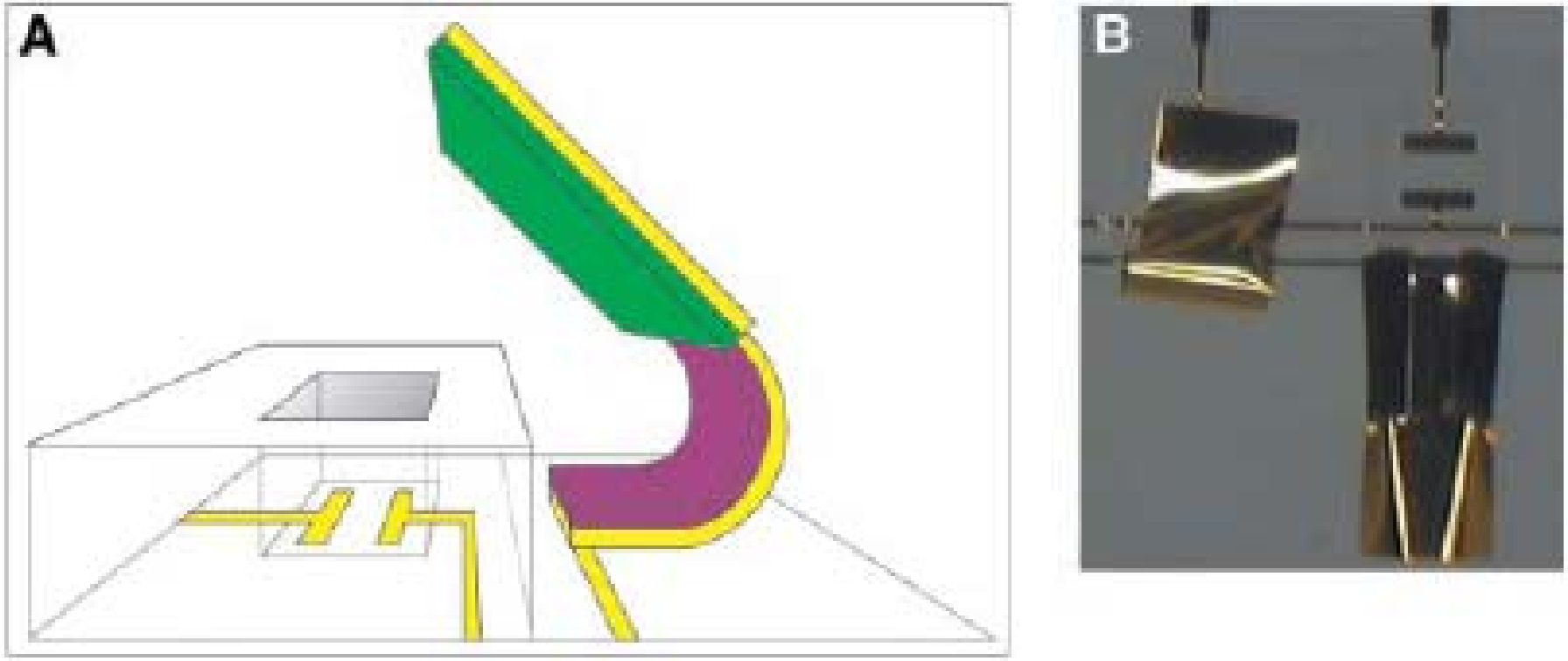

Figure 24.19 Micron sized hinge flap is one example of a polymer actuator – operated device suitable for biological applications. (From Jager, E.W., Smela, E., and Inganas, O., Science, 290, 1540, 2000. With permission)

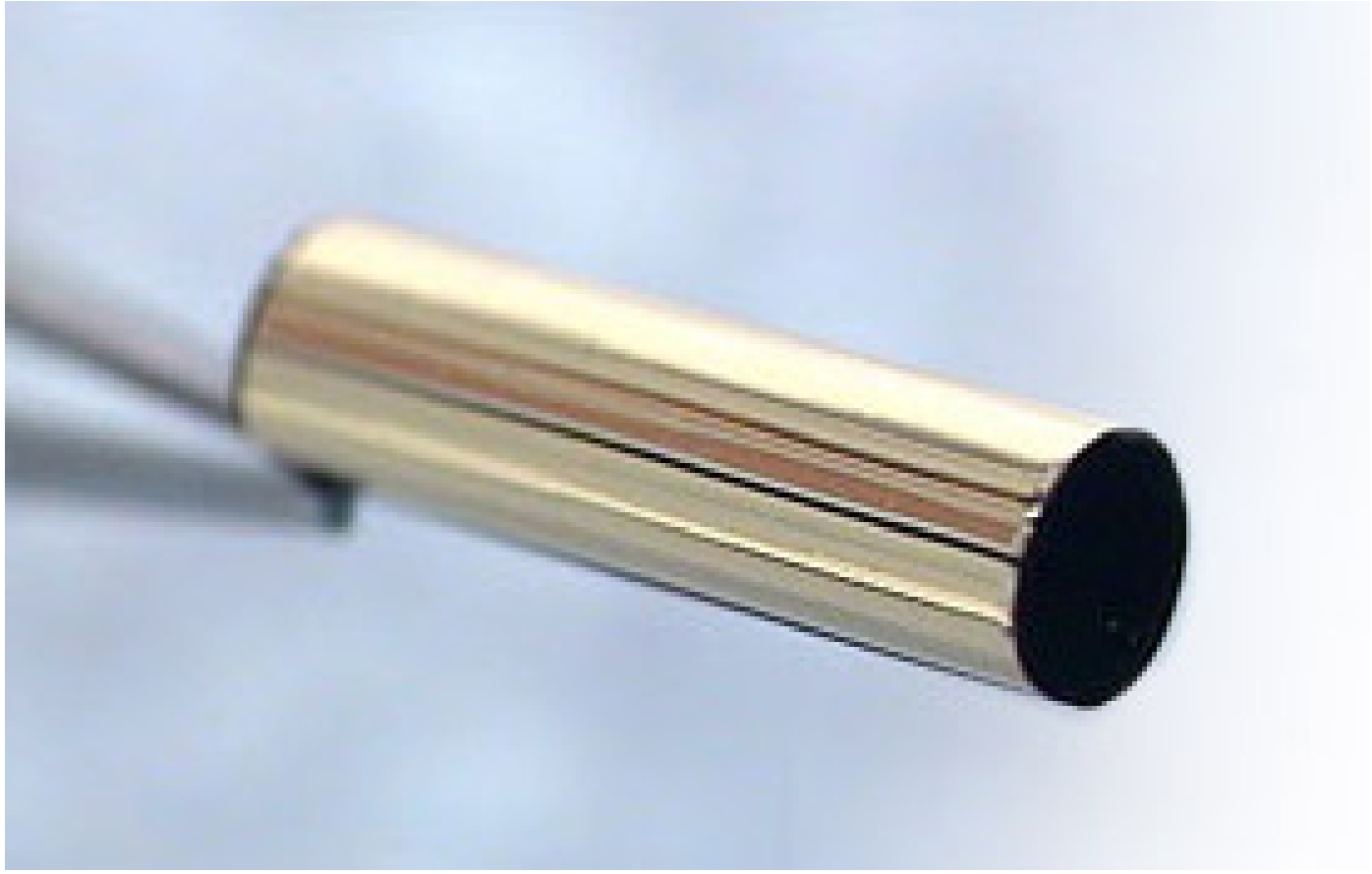

Figure 24.20 The connector for blood vessels, as developed by Micromuscle AB [64]. (From Micromuscle AB, Westmansgatan 29, SE-582 16, Linköping, Sweden, With permission)

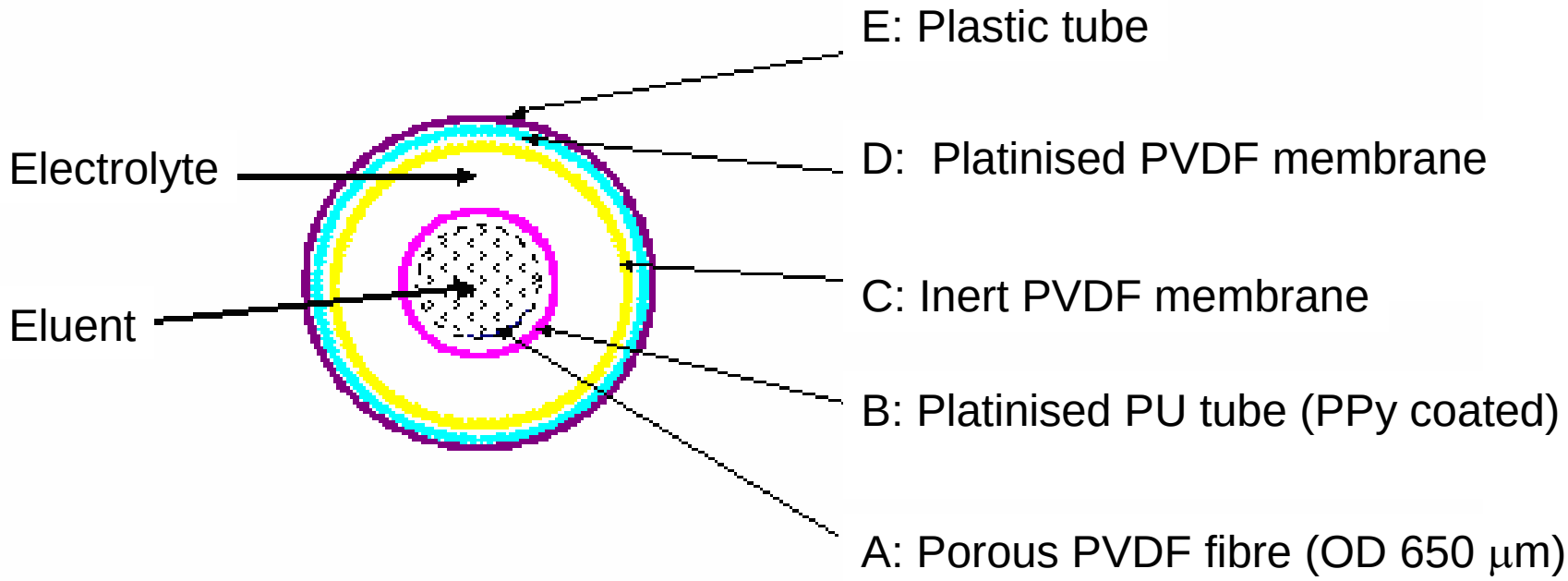

Figure 24.21 Schematic diagram of a tube-in-tube-actuator-nodule (TITAN) pump system [65]; A: porous PVDF fibre (outside diameter (OD): 650 μm) used to maintain the micropump cylindrical shape, B: platinised PU tube (OD: 1050 μm, inside diameter (ID): 950 μm) wrapped with Φ 50 μm platinum wire and coated with PPy, used as TITAN working electrode. C: inert PVDF membrane, used as an inert electrochemical cell separator and to hold the 0.25 M TBA•PF_6/PC supporting electrolyte, D: platinised PVDF membrane coated with PPy connected via stainless steel mesh, used as TITAN auxiliary electrode, and E: plastic tube (30 mm long, OD: 5 mm, ID: 4 mm) used to pack the electrode assembly. (From Wu, Y., Zhou, D., Spinks, G.M., Innis, P.C., Megill, W.M., and Wallace, G.G., Smart Mater. Struct., 14, 1511, 2005, With Permission.)

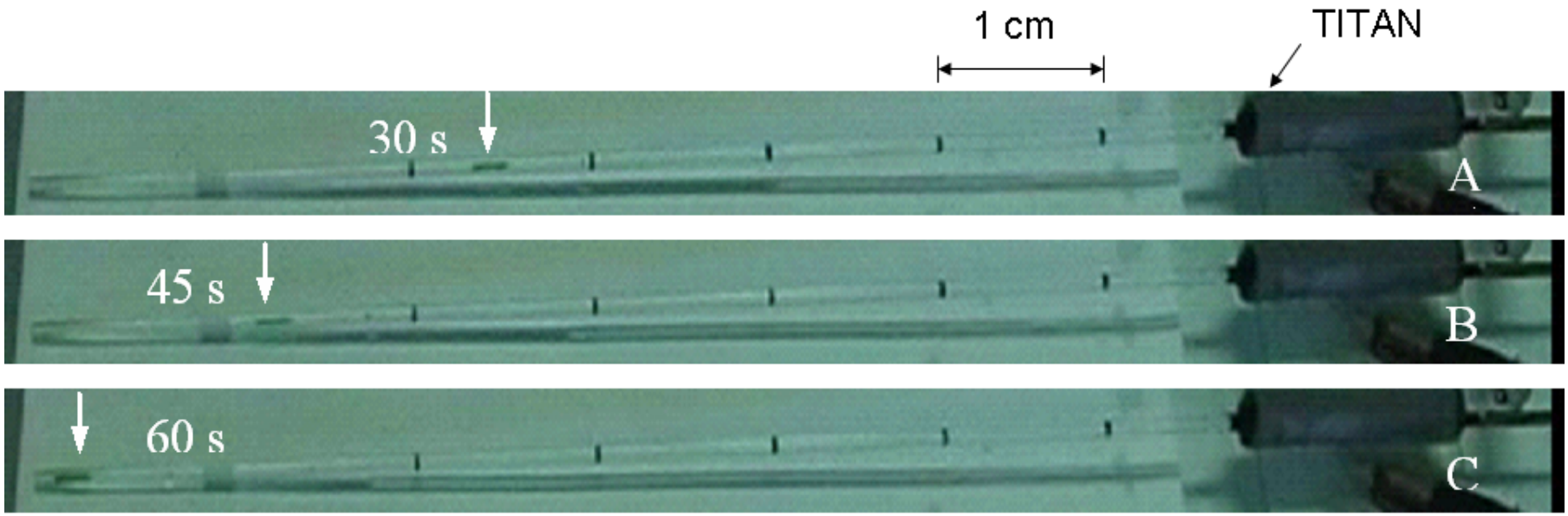

Figure 24.22 Sequence of video frames showing the displacement of dyed plug through an open-end glass capillary. (A) +1.0 V applied (0-30 s), TITAN working electrode expands and plug moves towards the pump, (B) voltage switched to –1.0 V (30-60 s), TITAN working electrode contracts and plug moves away from the pump, and (C) displacement reached after -1.0 V applied for 30 s.